Construction and Building Materials 371 (2023) 130730

Contents lists available at ScienceDirect

Construction and Building Materials

journal homepage: www.elsevier.com/locate/conbuildmat

Petrographic, microstructural and petrophysical study of asphaltic limestone employed in the Late Baroque towns of the Val di Noto UNESCO site (south-eastern Sicily)

R. Punturo [a,b,*], V. Indelicato [a], G. Lanzafame [a], R. Maniscalco [a], E. Fazio [a], A. Bloise [c], L. Muschella [a], R. Cirrincione [a]

[a] Department of Biological, Geological and Environmental Sciences, University of Catania, Corso Italia 55, 95129 Catania, Italy
[b] Institute of Environmental Geology and Geoengineering (IGAG—CNR), 00185 Rome, Italy
[c] Department of Biology, Ecology and Earth Sciences, University of Calabria, I-87036 Rende, CS, Italy

ARTICLE INFO

Keywords:
Pietra Pece (Pitchstone)
Fabric analysis
Hydrocarbon impregnation
Porosity
X ray micro-CT
Geomaterial
Hyblean Plateau
SE Sicily

ABSTRACT

Pitchstone is one of the building materials used in the monumental architecture of the late Baroque towns of the Val di Noto (UNESCO World Heritage Site) in the Hyblean Plateau (SE Sicily). Our research goal is to define the relationships between microstructural properties and bitumen impregnation, which confer the distinctive shades and excellent physical–mechanical properties to this valuable geomaterial. The study has been conducted by optical microscopy, synchrotron X-ray microtomography, ultrasonic testing, gas chromatographic analysis, differential scanning calorimetry and thermogravimetry investigation on two differently impregnated samples, representative of the main exploited and marketed pitchstone lithotypes. It revealed a close relationship between petrofabric and petrophysical properties, and impregnation amount.

1. Introduction

Also known as "asphalt" or "asphaltic rock", pitchstone is a limestone impregnated, in a percentage between 7 % and 10 %, with bitumen [1,2], i.e., a solid hydrocarbon resulting from the oxidation of liquid or gaseous hydrocarbon. In the present study, the affected lithotypes belong to the Hyblean succession, originally deposited in the time interval between the Triassic and Miocene and subsequently involved in deformation following the collision between the Africa and Europe plates [3]. Pitchstone, extracted from the Ragusa area in south-eastern Sicily (Italy) has been widely used over the centuries as a valuable stone material in construction, art and for hydrocarbon extraction. Particularly, this dimension stone has been used either for external architecture elements, like facades, or as ornamental material for interiors, due to the characteristics conferred by bitumen impregnations. Indeed, this lithotype displays particular chromatic shades (from black to brown with whitish streaks), excellent physical–mechanical features [4,5] such as insulating properties against rising damp [3], good erosion resistance. Although the use of pitchstone, as an ornamental material, dates back to ancient origins, the extraction or collection of bituminous stones in prehistoric times is difficult to prove. Insights of its ancient use derive from the discovery of rare artefacts [6], of which the most significant remains are several sarcophagi found in August 1891 C.E. during railway construction works and attributed by archaeologists to a period between approximately 2500 and 2200 years C.E. [7,8]. Recent geophysical survey [9] noticed buried structures beneath the Church of St. George in Ragusa Ibla, suggesting that many artifacts occur in the area. Even Teophrastus, in his text titled "*Peri* Lithon" (i.e. On Stones), mentioned the asphalt bearing rocks of the Hyblean area. Among historical artifacts, it is worth mentioning the statue of St John the Black, probably the oldest preserved work of art, dating back to the 16th century and hosted in the Cathedral of St John the Baptist (Fig. 1a), and a tombstone from 1577 C.E. (Fig. 1b) preserved at the Church of St. Francis at the Immaculate Conception; pitchstone was also used for the Church of St. George, (Ragusa Ibla) (Fig. 1c, d). The extensive use of asphaltic stone as an ornamental valuable stone material, however, is subsequent to 1693 C.E. earthquake that destroyed several towns and cities in south-eastern Sicily, among which Syracuse, Catania, Ragusa,

* Corresponding author.
E-mail addresses: rosalda.punturo@unict.it (R. Punturo), gabriele.lanzafame@unict.it (G. Lanzafame), rosanna.maniscalco@unict.it (R. Maniscalco), eugenio.fazio@unict.it (E. Fazio), andrea.bloise@unical.it (A. Bloise), ludovica.muschella@studium.unict.it (L. Muschella), r.cirrincione@unict.it (R. Cirrincione).

https://doi.org/10.1016/j.conbuildmat.2023.130730
Received 5 August 2022; Received in revised form 2 February 2023; Accepted 11 February 2023
Available online 27 February 2023

Noto, Modica, Scicli, Palazzolo Acreide and Avola. As a result of this catastrophic event, the territory reacted with an intense reconstruction activity [10,11] that led to the construction of buildings and churches characterized by the late Baroque architecture of the 18th century. Reconstructed towns have been recognized since 2002 as a World Heritage Site, the "UNESCO Late Baroque towns of the Val di Noto" [12]. Keeping within the Late Baroque style of the day, these towns and cities also display distinctive innovations in town planning and urban building [13]. Moreover, it is worth noting that some of the towns are subject to landscape protection (under the Italian Law 1497/39). A very common feature in these monuments of the Baroque period is the bichromy, due to the use of either magmatic rocks or black bituminous limestone in combination with whitish sedimentary rocks [11,14–17]. This also holds for the post-earthquake monuments of the city of Ragusa, where pitchstone, ranging from brown with whitish veins to almost black as the bitumen content increases, was used as an embellishment material in façade friezes, internal and external floors (Fig. 1c), staircases, church columns as an architectural pattern, and in funerary construction [6]. The magnificent Cathedral of St. George in Ragusa Ibla (Sicily) with its biochromatic façade is one of the most important Baroque monuments of eastern Sicily (Fig. 1d) [14,18–20].

The most involved sectors in the industrial processing of asphaltic rock were two: extraction of hydrocarbons to produce either lubricating liquid and fuel, and the paving of roads that, until then, were made of stone slabs [17]. The breakthrough for asphalt stone came in 1711 C.E. in Switzerland, when the Greek teacher Eirini D'Eyrinis, noticed that spreading a layer of this crushed asphalt stone on the roads made the pavement waterproof. It prevented also the formation of the summer dust caused by the passage of carts or the swampy ditches during rainy winters. Consequently, he began to market it [6,17]. At the time of the Kingdom of the two Sicilies (1816–1861 C.E.), the Ragusa district was one of the two largest Italian districts already partially exploited by local entrepreneurs for use as ornamental stone. After the establishment of the Kingdom of Italy (year 1861 C.E.) the industrial extraction by foreign companies began [6]. In particular, according to literature [17] the industrial extraction of asphaltic rock in Ragusa started in 1855 C.E. in the three hundred hectares of the mining area of Tabuna district, that included the so called Tabuna mine (Fig. 2a, b; Fig. 3) and the Castelluccio-Streppenosa mine. The exploitation of the mines of Ragusa provided an enormous amount of this strategic geomaterial which was used for road paving of many Italian and European cities such as Milan, Palermo, Berlin, Paris, Amsterdam, and London. Given the quality and the extension of the Ragusa oil field, all the mining area was considered meaningful and of strategic importance for the Italian industrial development [21]. During the Second World War, the rock extraction, and the production of by-products (oil, bitumen and road paving powder) were reduced to almost zero. Therefore, between 1943 and 1945, some local companies started a new cement factory in which the exhausted limestone (i.e. deprived of its oil content) was used for the production of pozzolanic cement [17] which became the main activity [1]. Currently, most of the mines and quarries of the Ragusa area are dismissed and testify to a grand monument of the Sicilian industrial archaeology. Nowadays, the study of the Hyblean bituminous limestones represents a great challenge for the construction industry in terms of efficient and sustainable (re)use of available georesources and in the context of circular economy. Provided its aesthetic appearance, which is of

Fig. 1. A) statue of st john the black (i.e. st john the baptist) originally from the church of Ibla which collapsed in 1693, now preserved in the Cathedral of Ragusa Ibla; b) 16th century tombstone (Church of St. Francis at the Immaculate Conception) Cathedral of St George, city of Ragusa Ibla (Sicily): c) Flooring; and d) Bichromatic façade of the church.

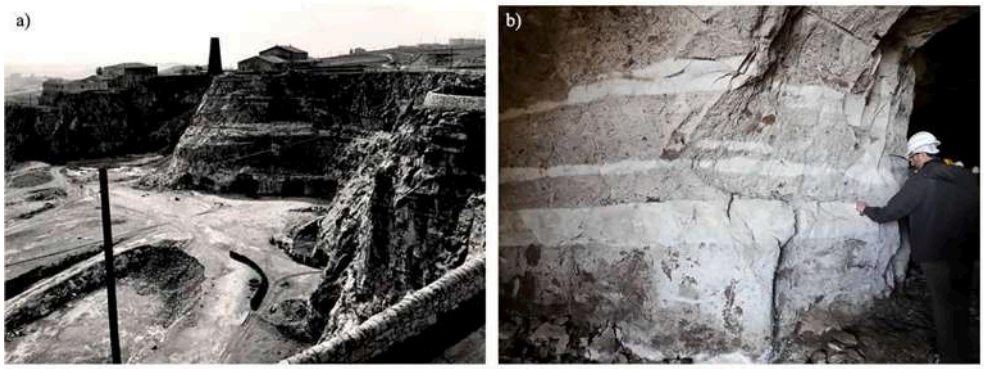

Fig. 2. Images depicting the asphalt mining area of Tabuna district with alternating layers of white and brown-black calcarenites, reflecting the different percentages of impregnation. In particular, the photo on the left (a) represents the quarry and gallery fronts in the 1950s (modified after [6]) and the photo on the right (b) shows the quarry in the present days.

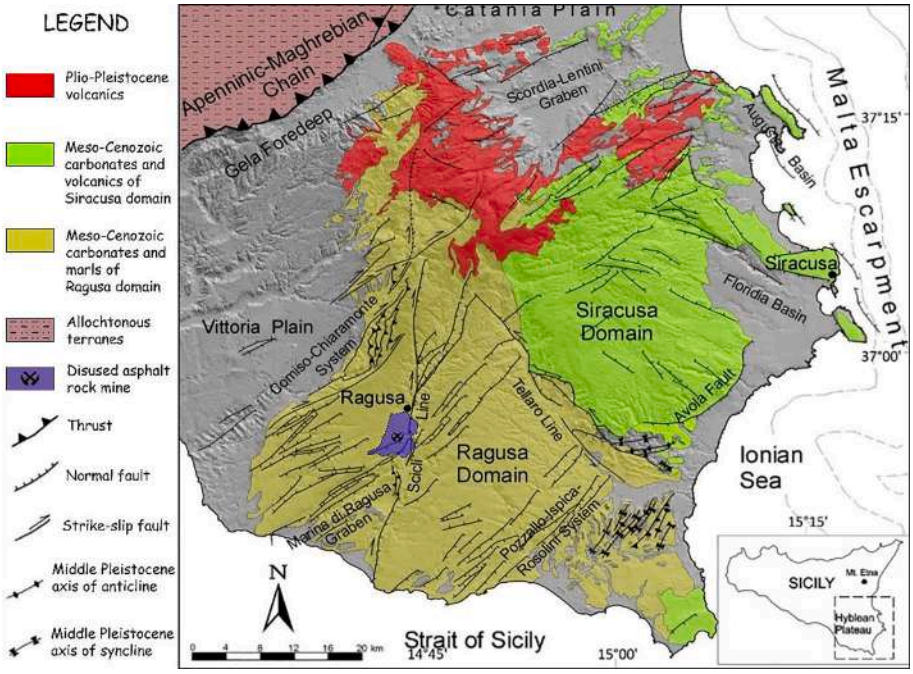

Fig. 3. Asphaltic basin of Ragusa with localization of the mining areas of Tabuna, district represented in yellow (modified after [55]). (For interpretation of the references to color in this figure legend, the reader is referred to the web version of this article.)

fundamental importance for its use as a valuable material, pitchstone has been the subject of several works, but mainly focussing on its exploitation for oil production or its use in monuments in a broader sense. Instead, the main aim of this study is to explore in detail the fabric-related rock properties by multi-analytical investigations to understand the relationships between petrological and petrophysical properties and bitumen impregnation and the link with its physical–mechanical properties and colour shades, Indeed, despite this rock has been employed for a long time as dimension stone, it was not studied in detail before. After this detailed knowledge, intervention on monuments as well as its proper use for flooring, cladding, and paving of buildings and monuments may be properly planned. At the same time, our work aims to shed new light about knowledge on hydrocarbon-bearing rocks, since the detailed knowledge of pitchstone may also tackle the urgency of stable and sustainable raw materials supply and availability, that may assure territorial independence in the European process of green transition.

2. Geological setting

Pitchstone samples were taken from the Tabuna Mine, located on the southern outskirts of the city of Ragusa (Sicily, Fig. 3). The Hyblean Plateau, in south-eastern Sicily (Fig. 4), is the emerged portion of the foreland domain [22], bounded to the east by the Malta escarpment, which separates the continental crust from the oceanic crust of the Ionian Sea [23,24], and to the west by the front of Apenninic-Maghrebian Chain, known as “Gela Nappe” [22,25]. The Hyblean Plateau is the culmination of the Mesozoic-Cenozoic carbonate sedimentary succession of a larger crustal sector, known as Pelagian Block, which geologically corresponds to the northern edge of the African plate [25–29]. Although the Hyblean Plateau is a foreland, it is strongly affected by faults. The main tectonic structures are NE-SW-oriented normal fault systems, with big offset, cutting the plateau towards the Gela Foredeep and a large-scale strike-slip fault system, oriented N10°-20°E, known as Scicli-Ragusa Line [27,30–32]. The age of this fault system is believed to be Cretaceous-Tertiary in age [31] reactivated in the Plio-Pleistocene, and with indications of recent reactivations

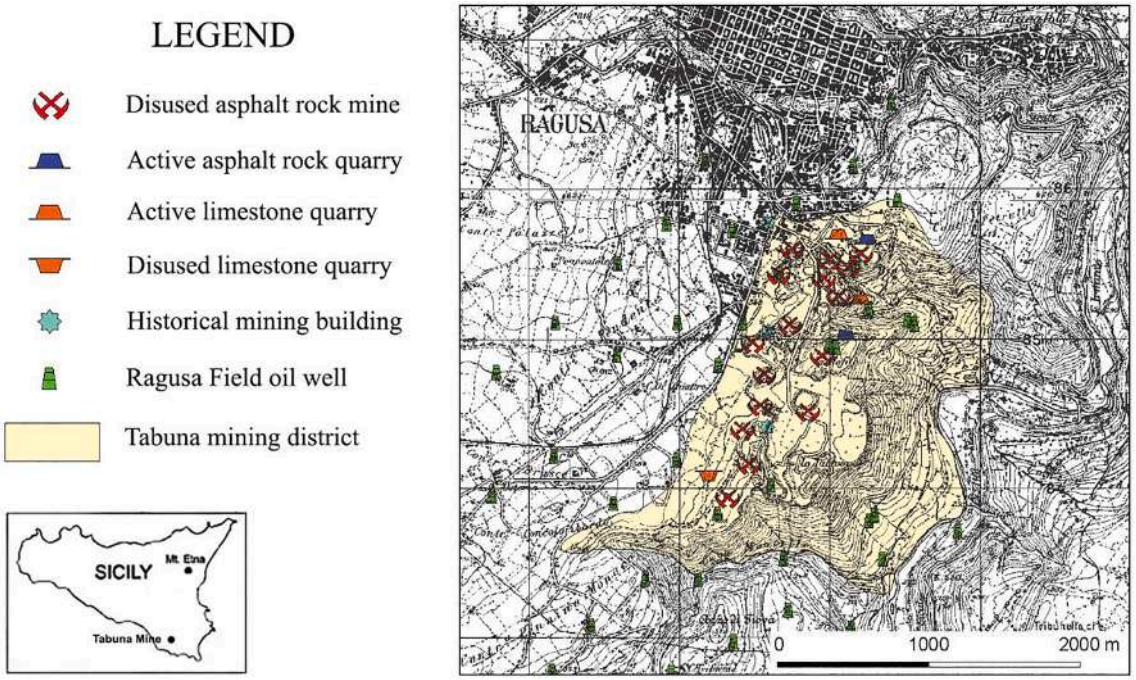

Fig. 4. Geological-structural map of the Hyblean Plateau showing the location of the Ragusa field oil wells and the mining area of Tabuna and Castelluccio-Streppenosa districts (modified from [32]).

[33,34].

From Cretaceous times onward, the Hyblean Plateau can be divided into two distinct sectors: the eastern and western (Fig. 4) [22]. The eastern Miocene succession consists of massive to thick-bedded carbonates and overlying reef to lagoonal limestones with intercalated pyroclastic rocks (Mt. Climiti, Palazzolo and Mt. Carrubba Formations). Instead, the western sector of the plateau is characterised by well-exposed upper Oligocene–Miocene limestone and marl deposited on a carbonate ramp under neritic to pelagic conditions (Ragusa and Tellaro Formations).

A substantial change in paleogeography is linked to the growth of upper Cretaceous volcanic seamounts in the eastern sector of the plateau, in both parts of the ancient Ragusa and Syracuse domains. During the Jurassic and the Cretaceous, volcanic activity occurred in the eastern part of the plateau and was probably related to extensional tectonics [22,25,28]. Volcanism probably had a prominent role on organic matter maturation, started in Late Triassic times in the Hyblean sector [35,36].

The distribution of bitumen mineralization mainly affects the basal rock levels of the Ragusa Formation, and in particular the Miocene Irminio Member, where the pitchstone mines sit on (see Fig. 5) [37]. The source rock is the Streppenosa Formation, deposited in a rapidly

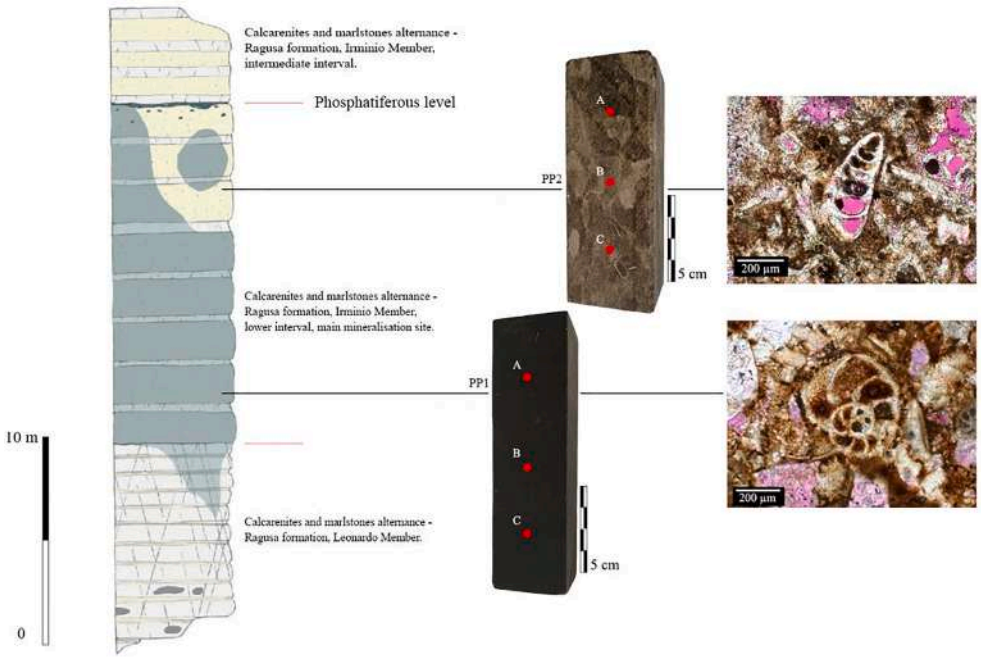

Fig. 5. Stratigraphic section of the Ragusa Formation in outcrop showing the position of samples PP1 and PP2 in relation to the different levels of impregnation. The larger impregnation of sample PP1, evident by its blackish colour, is also observed microscopically by the total filling of the bioclastic chambers. Sample PP2, on the other hand, shows its lower impregnation through the presence of residual porosity. The image also shows the points of P-wave velocity measurements (the red dots). (For interpretation of the references to color in this figure legend, the reader is referred to the web version of this article.)

subsiding basin under anoxic conditions and consisting of turbiditic grey-green dolomitic limestones with interbedded black shales [32] rich in organic matter. As a result of the interstitial pressures generated by the formation of oil from the kerogen, the oil was expelled from Streppenosa Formation and migrated through fractures, karstification and/or dissolution surfaces towards the reservoir rock represented by the lateral and underlying dolomites of the Noto formation. The Streppenosa Formation acted as both source rock and seal, but the ascent of liquid hydrocarbons from the deep oilfield takes place through the main discontinuities associated to Scicli-Ragusa Fault System (Fig. 4).

3. Materials and methods

3.1. Petrographic analysis of the stone samples

Two representative samples were taken from the Tabuna Mine, located in the southern part of Ragusa town, where the outcropping levels are characterized by an alternation of light and dark-coloured layers, whose shade was presumably related to the percentage of bitumen impregnation (Fig. 5). They both belong to the Ragusa Formation. The two samples, labelled PP1 and PP2, were taken respectively in a darker and a lighter layer in order to determine the differences in the fabric that may have influenced bitumen absorption and particularly the relationship between porosity and impregnation.

The petrographic analysis of the cross-sections of the samples was carried out to determine if the compositional and textural characteristics, in particular grain size, matrix, cement and porosity, could have influenced the bitumen absorption capacity. Thin sections of PP1 and PP2 were analysed using a Zeiss Axiolab polarizing optical microscope equipped with an Exacta + Optech camera (E3SPM), and a γ (or first-order red) compensator was used to highlight porosity. Images were acquired with MIImageView software [38] and subsequently processed.

3.2. X-ray computed microtomography investigation and 3D image analysis

A detailed study of the microstructural characteristics of the pitchstone samples was performed by synchrotron radiation X-ray computed microtomography (SR X-ray μCT) at the SYRMEP (SYnchrotron Radiation for MEdical Physics) beamline of the Elettra synchrotron (Elettra - Sincrotrone Trieste S.C.p.A, Trieste, Italy) in high spatial resolution white-beam configuration mode.

The X-ray spectrum was filtered for low energies with 1 mm of Si + 1 mm of Al, and the sample-to-detector distance was set to 200 mm. For each measurement, 1800 projections were acquired over a total scan angle of 180° with an exposure time/projection of 2 s. The detector consisted of a 16-bit air-cooled sCMOS camera (Hamamatsu C11440 22C, Hamamatsu City, Japan) with a 2048 × 2048 pixels chip. The effective pixel size of the detector was set at 1.952 μm^2, yielding a maximum field of view of ca. 3.22 mm^2. Since the lateral size of the samples (~4 mm) was larger than the detector field of view, the X-ray tomographic micro scans were acquired in local or region-of-interest mode [39]. Single distance phase retrieval-pre-processing algorithm [40] was applied to the white beam projections in order to improve the reliability of the quantitative morphological analysis and enhance the image contrast.

The reconstructed 3D images were then processed by Fiji software [41] to extract binary images of the phases of interest (pores and bitumen) and by Pore3D software library [42,43] to retrieve their abundance and morphology. The distribution of the pore size was calculated as Pore Number Density (PND) and Pore Volume Density (PVD) [44]. The PND is obtained dividing the number of pores with a determined size range for the total number of pores of the sample, whereas the PVD is calculated as the sum of the volumes of the pores of a given size range divided by the total volume occupied by porosity.

The 3D visualization was performed by VGStudio 2.2 software (Volume Graphics, Charlotte, NC, USA) [45].

3.3. Ultrasonic testing

P-wave propagation velocity in rock samples was determined using the 24-bit M.A.E. (Molise Electronic devices) A5000M ® data acquisition system, equipped with 53 kHz transducers placed according to the direct method. The device consists of a pulse generator, equipped with 53 kHz transducers and an electronic counter for time interval measurements. Since both rock sample do not exhibit any visible fabric anisotropy, the parallelepipeds were cut along three arbitrarily chosen directions (length: ca 50*50*150 mm).

Before testing, the samples were first washed with deionized water and then placed in an oven to dry at low temperature, approximately 40 °C, to evaporate all the water content (i.e., until constant mass conditions were reached). Subsequently, they were placed in a desiccator, containing silica gel capable of absorbing moisture, until cooled.

After calibrating the instrument, the transit time (Δt) was measured in both parallelepiped PP1 and PP2 samples both longitudinally and at three transverse points. The distance between transducers at each measurement point was determined by calliper.

From the transit time measurement [46,47], it is possible to calculate the P-wave propagation velocity using the following equation:

$$V_P = l/\Delta t; [km/s]$$

Where:

- Vp is the P-wave propagation velocity at each measurement point;
- l is the edge length, corresponding to the distance between the two transducers;
- Δt is transit time of the compressive sound wave trough the sample.

Elastic wave velocity measurements were carried out according to the ASTM, D 2845–2000 [48] indications. Moreover, measurements along three mutually perpendicular directions on parallelepiped (arbitrarily cut since the lithotypes do not exhibit any anisotropic fabric elements such as foliation) permitted to calculate the seismic anisotropy, defined after [49] as

$$A\% = (Vp_1 + Vp_2 + Vp_3)/Vp_{mean}*100.$$

3.4. Gas chromatography analysis

The gas chromatographic analysis was performed on the oils extracted from the two samples PP1 and PP2 to quantify the hydrocarbons contained in the rock porosity. To extract the oil, the samples were previously ground with a mechanical press and sieved with a 2 mm sieve at the University of Catania. Oil extraction and gas chromatographic analysis were performed at ARPA Sicily (Sicilian regional agency for environmental protection). About 5 g of the sieved PP1 and PP2 samples were diluted with 40 cc of hexane. The mixture was then placed in ultrasonic baths for 20 min using Bandelin SONOREX™ Digital 10 P Ultrasonic baths (DK 1028 P, capacity 28 L) and filtered with anhydrous sodium sulphate to retain water. The process was repeated on the residues twice. 30 g of Florisil® were added to purify the obtained raw, then the mixture was placed on a horizontal shaker (ASAL, mod. 709/O) for 30 min, after which the solution was filtered again using filter paper in folded discs. To evaporate the solvent, the small volume reduction was performed through a thermal bath at 40 °C using the LabTech Rotary Evaporators EV400 touch.

The reduction collected by rinsing the flask with hexane was placed in the vials and dried using a ScanVac Vacuum Concentrator Scan Speed at −53 °C and an operating speed of 2000 rpm for 30 min. The vials had previously been brought to constant weight using the desiccator. This extracted 0.0557g of oil for PP1 and 0.0488g for PP2.

Determination of C12 to C40 hydrocarbons on oils extracted from

asphaltic rocks PP1 and PP2 was performed through a Thermo Scientific TRACE GC Ultra™ equipped with the Thermo Scientific TriPlus™ autosampler. The gas chromatography capillary column has a diameter of 0.1 mm and a length of 10 mm. Hydrogen is used as a carrier gas for analytes in the column with a constant flow rate of 0.5 ml/min. In the sequence of analysis, the petroleum ether was injected twice: the first time to clean the system, the second time to calibrate the blank in the chromatogram. Acquisition was performed in a temperature range from 50 to 350 °C, with isotherms every-two minutes and a heating rate of 35 °C/min. The injector used was a Split/Splitless type, with a split ratio of 20 and at temperature of 300 °C. Lastly, the detector temperature was maintained at 350 °C. The calibration standard used to create the calibration line was BAM CRM 5004 diesel fuel/lubricating oil (1:1), certified on a mass ratio basis. The range of detectable hydrocarbons depends on the calibration standard used, i.e., BAM CRM 5004 diesel fuel/lube oil (1:1). The calibration line ranges from 0.1 mg/ml to 10.0 mg/ml, therefore the oils extracted from the sample were diluted in 10 ml of petroleum ether to obtain a detectable concentration of 5.57 mg/ml for PP1 and 4.88 mg/ml for PP2, respectively.

3.5. Thermogravimetry (TG–DTG) and differential scanning calorimetry (DSC)

Differential Scanning Calorimetry (DSC) and Thermogravimetric Analysis (TG) were performed in an alumina crucible under a constant aseptic air flow of 30 ml min^{-1} with a Netzsch STA 449 C Jupiter in a 25–1200 °C temperature range, with a heating rate of 10 °C min^{-1}. Approximately 30 mg of sample were used for each run [50]. Instrumental precision was checked by five repeated collections on a kaolinite reference sample revealing good reproducibility (instrumental theoretical T precision of ±2 °C) with DSC detection limit <1 μW. Derivative thermogravimetry (DTG), derivative differential scanning calorimetry (DDSC), onset, exo- and endo-thermic peaks were obtained using Netzsch proteus thermal analysis software. It is worth mentioning that the curve of Differential Scanning Calorimetry (DSC) characterizes the heat effects related to physical and chemical conversions of samples, the thermogravimetric (TG) curve shows the weight variation of the sample during heating; the differential-thermogravimetric curve DTG characterizes the rate of weight variation of the sample during heating.

4. Results and discussion

The petrophysical properties of carbonate rocks (porosity, permeability) are strictly related to their genesis, changing according with the nature, organization and shape of their constituents (e.g. grains, pores, cement, minerals), and diagenetic evolution [32,51–53]. These properties are also strongly influenced by the presence of the tectonic discontinuities, mainly consisting of cracks, veins, stylolites fractures and microfaults [54,55], affecting the different carbonate lithotypes. For this reason, the two specimens, representative of the pitchstone lithotypes varieties were first investigated through macroscopic observation, to outline their main characteristics and provide a first classification and, subsequently, through a microscopic analysis, to better delineate their fabric-related properties. The geological stratigraphic location and the mesoscopic and microscopic main features are shown in Fig. 5.

Sample PP1 is black and homogeneous and is characterized by an intense bitumen smell and a greasy feel to the touch, indicating that the expected bitumen impregnation is quite large. Carbonate grains, most evident along the basal sections, range in size between 2 mm and 1/16 mm and therefore the rock can be roughly classified as *fine calcarenite*.

Sample PP2, on the other hand, exhibits a non-homogeneous brownish coloration, characterized by the spotted presence of creamy-colored veins. Therefore, the expected impregnation is lower than in sample PP1, the bitumen smell is less intense and the impregnation is weakly perceptible by touch. By considering the granulometry and the origin of the clasts, also this specimen can be classified as *fine calcarenite*. More specifically, as a result of microscopic observation of the fabric-related characteristics, the two samples can be classified as *packstones* according to Dunham [56] or as *packed biomicrite* according to the classification by Folk [57].

Petrographic investigation was carried out on thin sections obtained from the two fine calcarenite samples.

Microscopic observations revealed that both samples are similar in terms of mineral content, being composed of carbonate grains and bioclasts, and bitumen. In both PP1 and PP2, the fabric consists of fossil fragments, present roughly over 50 vol%, in a predominantly micritic matrix with a lower percentage of sparite, with calcite granules ranging in size from 0.02 to 0.1 mm; the bitumen mineralization is either interparticle (micrite voids) or intraparticle (bioclast, e.g. foraminifera chambers, Figs. 6 and 7). Based on the presence of *Globigerinoides trilobus* it possible to assign both samples an age not older than Early Miocene. Additionally, the presence of *Heterostegina* sp. in association with other benthic foraminifera, algae and echinoids suggests water depths of the order of 40 to 60 m, probably extended to depths of ~70 m; the depositional palaeoenvironment can be therefore referred to a carbonate ramp. Samples differ in average grain size, in the relative abundance in sparitic calcite and in the fossiliferous content. In particular, sample PP1 has overall larger grain size compared to sample PP2 and, consequently, a larger pore size also visible through 3D reconstructions. This sample also shows a slightly higher sparite content. The faunal content consists mainly of benthic foraminifera (of the suborders *Rotaliina, Miliolina, Textulariina*), planktonic globigerinids, bryozoans, sponge spicules and spicules of echinoderms (Fig. 7a, c).

In contrast, sample PP2 displays a slightly lower grain size and pore amount (Fig. 7b, d), a lower percentage of sparite and the fossil content consists of remains of benthic foraminifera, planktonic globigerinids, bryozoans and algae.

From a petrophysical point of view, porosity is a fundamental parameter for the study of the rock behaviour. It is in fact an intensive property that, in the case of reservoir rocks, describes the storage capacity of geofluids of the rock [46,47,52]. Porosity can be primary, i.e. present in the rock since the time of deposition, or secondary, when developed as a result of diagenesis. Moreover, pores can communicate or not, affecting the permeability of the rock and thus its ability to be impregnated by geofluids.

In the studied pitchstone samples, either primary intraparticle porosity (i.e. bioclast foraminifera chambers not filled by micrite or bitumen mineralization) and secondary porosity, of a dissolution type concentrated on calcite crystals, were observed. Sample PP2, in addition to having a smaller grain size of the clasts and pores, has a higher degree of primary porosity than that observed on section PP1. This is related to a lower filling of the bioclast chambers by micrite and bitumen mineralization (Fig. 7b, d). Conversely, the secondary porosity on calcite crystals is lower than that observed on sample PP1, most likely due to the lower presence of *sparite*.

In terms of impregnations, optical microscope analysis of the samples has shown that bitumen mineralization affects both the interparticle micrite and the bioclasts' chambers, which represented primary porosity at the time of deposition. Sample PP1 appears to be affected by increased impregnation, resulting in a decrease of residual primary porosity, which remains higher in the less impregnated sample PP2.

The image analysis of 3D volumes (by SR-CT) allowed to visualize the three-dimensional distribution of pores, grains and bitumen impregnation within selected samples and to perform quantitative analysis to retrieve the abundance of these phases (Table 1). The results obtained through image processing (Fig. 8a–f) agree with what has been observed so far: the percentage of bitumen is 22 vol% in PP1 and 17 vol % in PP2, and the estimated total porosity is 19 % and 24 % respectively. Therefore, the lower impregnation of PP2 results in a higher residual unfilled porosity. The image analysis of 3D volumes by SR-CT also permitted to quantify the grain size distribution within each specimen. Results indicate that grains have size between 2 and 400 μm, with

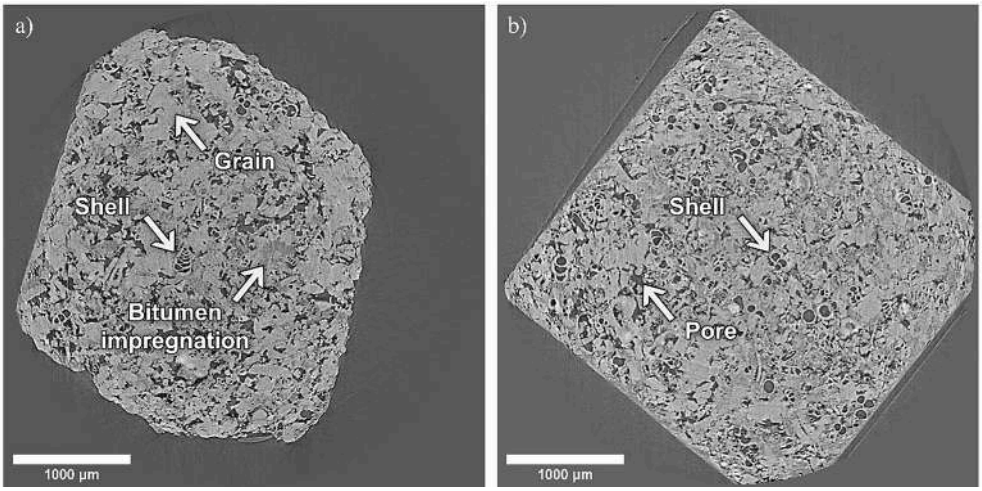

Fig. 6. SRμCT slices of sample PP1 (a) and PP2 (b) where pores and voids (very dark blackish grey), carbonate grains and shells (light grey) and bitumen impregnations (dark grey) can be distinguished.

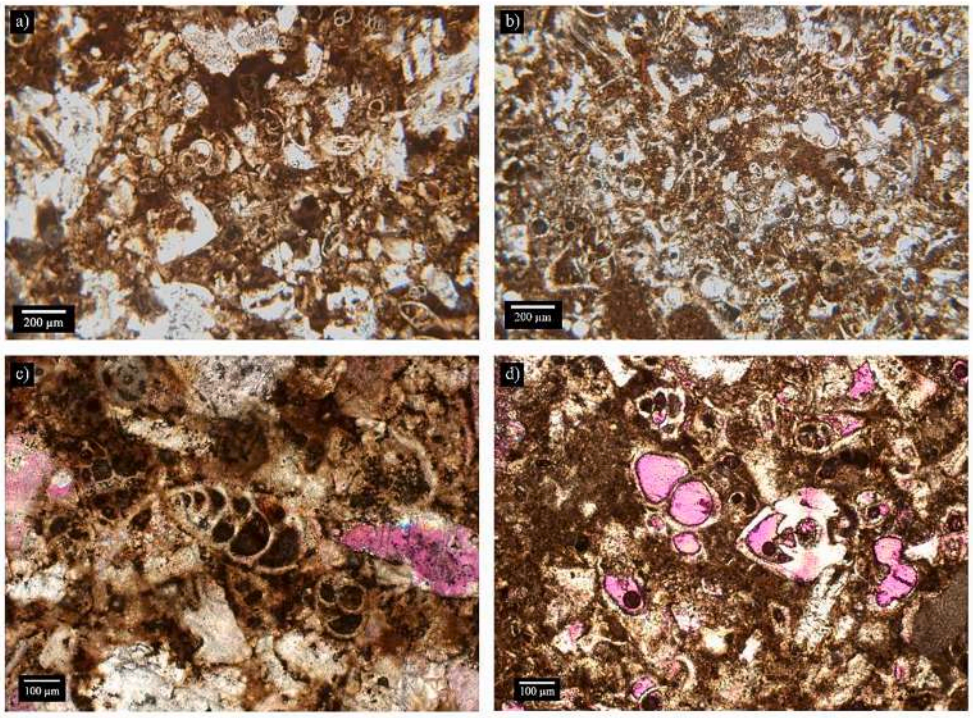

Fig. 7. Microscopy observations. Photomicrographs (a) and (b) show the fabric-related properties of samples PP1 and PP2, respectively. Sample PP1 (a) has a slightly coarser grain size than sample PP2 (b); photomicrographs (lower polarizer). (c) and (d) show the distribution of the impregnation in sample PP1 and in sample PP2, respectively; c) and d): crossed polarizers and with a gypsum additional compensator, which gives the pores the pink-magenta color. (For interpretation of the references to color in this figure legend, the reader is referred to the web version of this article.)

Table 1
Results of quantitative analysis on 3D images of pore and impregnation phase.

		Pores				Impregnation
Sample	Investigated Volume (mm^3)	Number density (#/mm^3)	Specific Surface (mm^{-1})	Amount (vol.%)	Average Volume (mm^3)	Amount (vol.%)
PP1	7.42	15,992	43.95	19.21	0.0000120	22.14
PP2	8.95	12,864	58.04	24.28	0.000019	17.23

similar distributions as shown in Fig. 9a. The grain number distribution indicates a slight prevalence of larger grains for PP1 with respect to PP2, with peaks at size of 146–166 um for PP1 and at 126–146 um for sample PP2. The distribution of the pore size, calculated as Pore Number Density and Pore Volume Density (Fig. 9b, c) does not show differences between the two samples, but remarks a high variability of the pore size that spans from few tens of μm^3 to few mm^3 in volume. Fig. 9b displays the prevalence of small pores (between 10^{-7} and 10^{-6} mm^3) that account only for a very small fraction of the total porosity (Fig. 9c). The large part of the porosity is indeed given by few but large (mm^3) pores that constitute >90 % of the voids of both PP1 and PP2 samples (Fig. 9b, c).

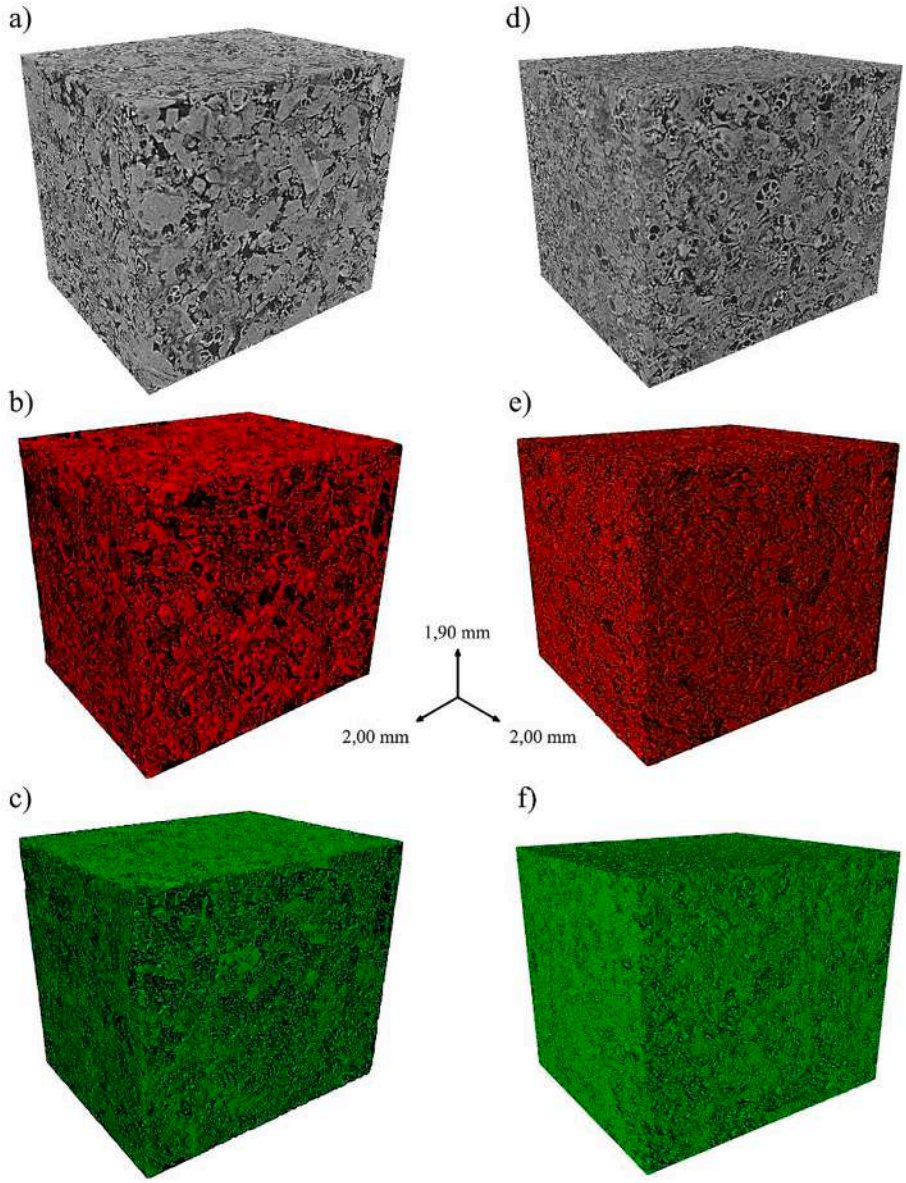

Fig. 8. 3D rendering of a selected part of the two samples analyzed by X-ray microtomography with synchrotron radiation: the images lined on the left represent the total solid volume (a), pore volume, 19% (b) and impregnation volume, 22% (c) for sample PP1; likewise, the images lined on the right represent the total solid volume (a), pore volume, 24% (b) and impregnation volume, 17% (c) for sample PP2.

Moreover, the velocity of the compressional wave is a function of either fabric features and of voids, microfractures and fluids (e.g. water, gas, oil, kerogen) [2]. The analysis reveals average P-waves velocities, respectively obtained for PP1 and PP2, of 3,63 km/s and 3,85 km/s. Specifically, the calculated P-wave velocity at each measurement point was: 3,33 km/s (longitudinal), 3,58 km/s (A), 3,58 km/s (B), 4,04 km/s (C) for PP1 and 3,40 km/s (longitudinal), 4,02 km/s (A), 4,03 km/s (B), 3,94 km/s (C) for PP2 (Fig. 5). The two specimens are also characterized by different values in seismic anisotropy ($AVp\%_{PP1} = 11.2$ %; $AVp\%_{PP2} = 17.6$ %). These results suggest that the investigated samples exhibit quite similar compositional content, whereas the fabric and microstructural features are responsible of small differences in seismic anisotropy, that can be attributed to the pore or microgranule local arrangement. Indeed, no significant fabric-related anisotropy (e.g. preferred orientation of grains, aspect ratio) was noticed in the samples. As far as the hydrocarbon content, gas chromatographic analyses were performed to quantitatively determine the presence of C12 to C40 hydrocarbons in the mineral oil extracted from samples PP1 and PP2 (Fig. 10a).

The obtained chromatograms show a concentration of C12 to C40 hydrocarbons in the extracted oils of 3.5410 mg/ml in PP1 (Fig. 10b) and 2.9986 mg/ml in PP2 (Fig. 10c). Therefore, considering the concentration obtained in the oil, which was previously diluted in 10 ml of ether, and the initial weight of the sample, it was possible to determine that the amount of hydrocarbons per kilogram in PP1 is 7,011.8 mg/kg and in PP2 is 5,997.2 mg/kg. Results from the thermogravimetry (TG–DTG) and differential scanning calorimetry (DSC) are represented in Fig. 11. Thermogravimetry (TG) has been used mainly to study the thermal stability of asphaltic limestone [e.g., [58–61]. The thermograms of the two asphaltic limestone were similar (Fig. 11a, b). In the TG curve, the initial weight loss observed up to 110 °C due to adsorbed water. Other than that, two different ranges of mass loss can be recognized. The first step (150–500 °C) is caused by a loss of volatile hydrocarbons. The second step between 700 °C and 900 °C is related to the decarbonation of calcite (mass loss of 39 %) in agreement with literature [47]. Overall, the TG curves for both asphaltic limestone samples (Fig. 11a, b) showed

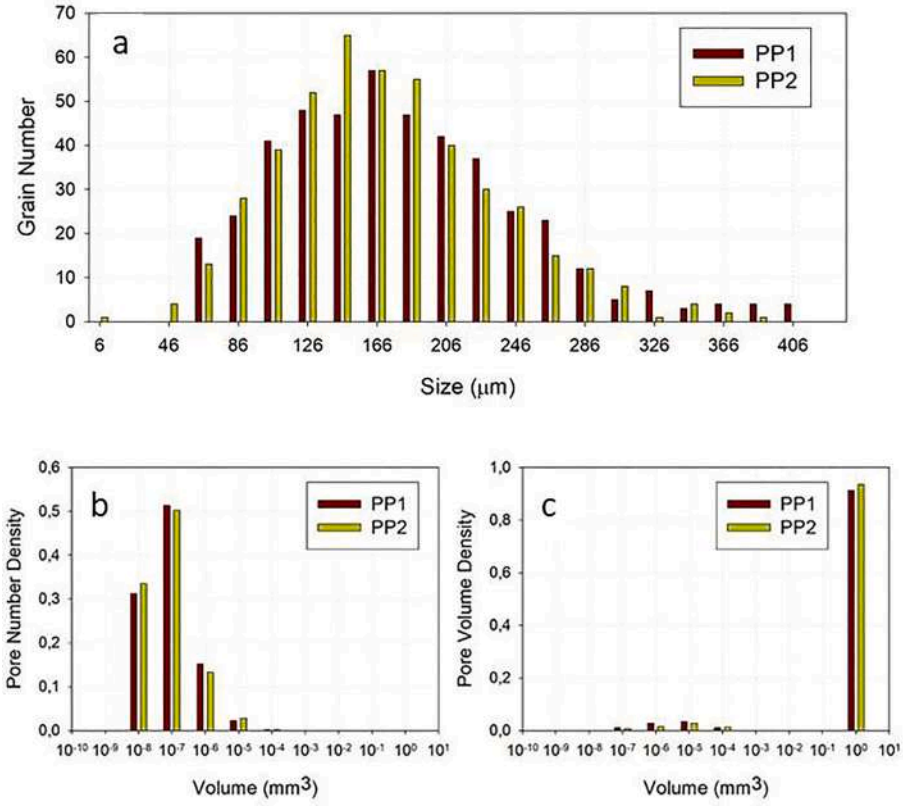

Fig. 9. Quantitative analysis of the two samples on the basis of X-ray microtomography with synchrotron radiation. a) Grain size distribution; b) pore number density and c) pore volume density.

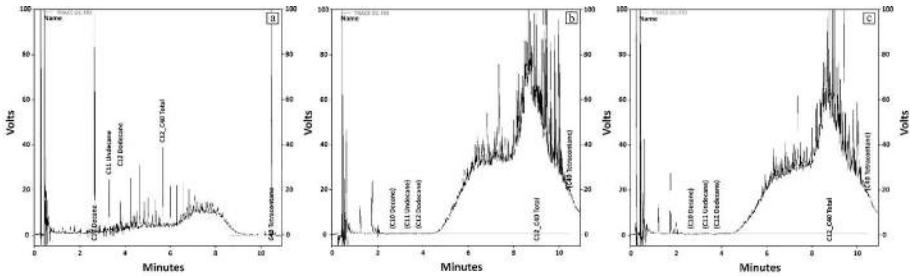

Fig. 10. Gas chromatogram of the calibration standard BAM CRM 5004 consisting of equal parts of diesel fuel and lubricating oil (a), and the C12-C40 hydrocarbon fractions of the oils extracted from the asphalt stone specimens: the concentration is 3.5410 mg/ml in PP1 (a) and 2.9986 mg in PP2.

a continuous weight loss (51 %) due to decomposition of first hydrocarbons and then calcite in the range 25–1200 °C. In the first step (110–600 °C) asphaltic limestone lose about 11 % of mass (Table 2) due to the liberation of hydrocarbons to produce coke. Indeed, at temperatures higher than 500 °C the most complex aromatic systems remain as non-volatile residue normally called coke [57]. DSC confirms the presence of hydrocarbons showing the exothermic peaks at about 350 and 440 °C on the DSC curves (Fig. 11a, b) as expected for oxidation [58,60,62]. The oxidation takes place with heat liberation and the exothermic effect is thus recorded on the DSC curve due to the reactions between oxygen and hydrocarbons. Hydrocarbons breakdown temperatures correspond to the point where oxidation is completed i.e., from ambient to 500 °C. Finally, DTG curves indicated the effect of asphaltic limestone samples studied. DTG showed three maximum loss rate at about 290, 350 and 440 °C ascribed to the liberation of hydrocarbons (see Fig. 11a, b). Peak temperatures, where the maximum rate of decomposition occurs, were established from DTG curves for both samples and are reported in Table 2.

Fluids flow is strictly influenced by the petrophysical properties of the lithotype. In general, organic-rich rocks are characterized by higher porosity, higher sonic transit time, lower density, higher γ-ray, and higher resistivity than other rocks [2,63]. Thus, in order to verify the petrophysical properties (porosity, seismic wave propagation), thin sections analysis, synchrotron radiation X-ray permitted to highlight the fabric-related petrophysical properties, also in terms of hydrocarbon content.

As far as the relationship between porosity and impregnation, the combination of polarised light microscope observations and microtomographic reconstructions highlighted their relationship. Indeed, the open porosity observed in PP1 results in fact approximately 19 vol%, compared to 24 vol% in PP2. Furthermore, the impregnation rates of ~22 vol% for PP1 and ~17 vol% for PP2 also agree with the porosity values: the higher impregnation of PP1 corresponds to a lower residual open porosity, as porosity is also intraparticle, and vice versa. This confirms the relationship between microstructural properties and impregnation, which results in the different macroscopic appearance of

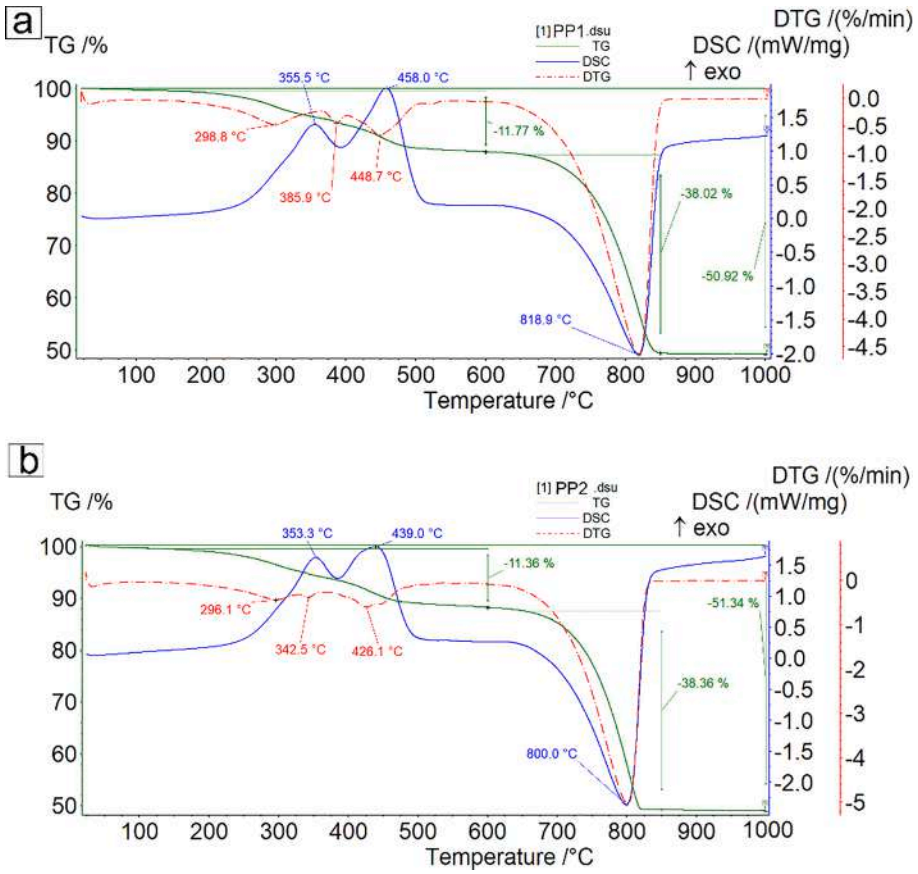

Fig. 11. Thermogravimetric results: a) derivative thermogravimetry (DTG) and b) derivative differential scanning calorimetry (DDSC).

Table 2
DSC and DTG peak temperatures and mass loss for both samples (PP1 and PP2). exo = exothermic; endo = endothermic.

Sample	DSC peak (°C)	DTG maximum loss rate peak (°C)	Mass loss (%)
PP1	335 exo	299	12 % in the range (110–600 °C)
	458 exo	386	38 % in the range 650–850 °C
	819 endo	449	51 % in the range 25–1200 °C
		819	
PP2	353 exo	296	11 % in the range 110–600 °C
	439 exo	342	38 % in the range 650–850 °C
	800 endo	426	51 % in the range 25–1200 °C
		800	

the samples. Previous studies on the façade of the Church of St. George in Ragusa Ibla (Fig. 1d) demonstrated the disappearance of bichromy as a consequence of photo-alteration on asphaltene inside pitchstone that leads to periodic restoration interventions [14,64], highlighting the need to characterize the employed construction materials. Moreover, the same authors [65] reported a high porosity (sometimes higher than 28 vol%) of the same asphalt-bearing calcarenite taken from the façade.

In general, the fabric-related as well as petrophysical properties of the Hyblean limestone types employed in the late Baroque cities of Val di Noto (e.g. [11,16,66,67] are different each other, also in terms of behaviour to weathering, especially when used in the monuments and architecture. The features of Ragusa pitchstone, characterized by average values of hardness of ca. 40kN/mm^2; compressive strength ca. 25.5 kN/mm^2 and flexural strength of ca. 6,5 kN/mm^2 [5,68], together with acoustic insulation features, suggest its reconsideration for new exploitation management. Indeed, this stone provides good insulation against rising damp, is characterized by good erosion resistance and is easy to work.

In addition, a comparison with the P-wave velocity values obtained by [32] on asphaltic limestones taken from the Eureka oil well, not distant from the Ragusa mining area (Fig. 4) and attributed to the Noto Formation (different in age, fossil content and fabric), showed that these carbonate reservoir lithotypes are also different in terms of elastic behaviour and porosity. Indeed, it has been seen that in the limestone of the Noto Formation, the pore plus impregnation system is often distributed along planes that can be mineralized micro-faults and veins. Conversely, pitchstone of Ragusa Formation is characterized by higher Vp and porosity values, and by the absence of stylolites and of other tectonic structures (e.g. micro-faults and veins).

5. Conclusions

The results of the multi-analytical investigation on the Pietra Pece (i.e. Pitchstone) of Ragusa (Sicily, Italy), a lithotype employed in the monumental architecture of the Late Baroque towns of the Val di Noto UNESCO list can be summarized as it follows:

- The two samples consist of fossil fragments, bioclasts, and carbonate grains in a predominantly micritic matrix (microcrystalline calcite) with a lower percentage of sparite. The mineralogical assemblage of the specimens consists of carbonate minerals (mainly calcite; the clasts mainly consist of microfossils and bitumen;

- In terms of seismic behaviour, the samples are characterised by comparable average P-wave propagation velocity values (3.63 km/s in PP1 and 3.85 km/s in PP2) that can be interpreted as the effect of the similar fabric of the two samples; nevertheless, since both lithotypes do not exhibit any observable fabric anisotropy, the noticed differences in seismic anisotropy may be due to the arrangement of pores and voids;
- C12-C40 hydrocarbon concentrations are higher in PP1 sample than in PP2 and can be related to the higher impregnation revealed by X-ray microtomography (22 % for PP1, compared to 17 % for PP2). This, together with the larger grain and pore size observed in PP1, allows us to conclude that the bitumen impregnations in these samples depend entirely on the pristine porosity properties.

Finally, our multi-analytical study succeeded in highlighting the intrinsic properties of an important valuable rock. Pitchstone turns out to be an excellent building material thanks to the presence of bituminous impregnation that gives excellent physical–mechanical properties (i.e. the good insulation against rising damp, good erosion resistance, malleability and workability).

Nowadays, the use of pitchstone is mainly suggested for interior design elements such as flooring, stairways, tiles for cladding, inlay elements, washbasins and counter tops, and also small objects such as trays, boxes, candle holders, soap dishes and similar.

In conclusion, in the context of circular economy and resources efficiency policy of Europe [69], asphalt bearing limestone from south-eastern Sicily may play a strategic role not only in the local economy, but also in the societal progress in terms of sustainable building and construction geomaterials, design, restoration and maintenance, as well as in monitoring available raw materials and planning their sustainable use in the context of green transition.

CRediT authorship contribution statement

R. Punturo: Conceptualization, Data curation, Funding acquisition, Investigation, Methodology, Supervision, Validation. **V. Indelicato:** Formal analysis, Data curation. **G. Lanzafame:** Formal analysis, Investigation. **R. Maniscalco:** Conceptualization, Funding acquisition, Investigation, Supervision, Validation. **E. Fazio:** Formal analysis, Data curation. **A. Bloise:** Formal analysis, Investigation, Methodology. **L. Muschella:** Formal analysis. **R. Cirrincione:** Conceptualization, Validation.

Declaration of Competing Interest

The authors declare that they have no known competing financial interests or personal relationships that could have appeared to influence the work reported in this paper.

Data availability

Data will be made available on request.

Acknowledgements

The authors are grateful to Ing. Nunzio Tumino, Colacem S.p.A., Director of Tabuna Mine, ARPA Sicily (Sicilian Regional Agency for Environmental Protection- Laboratory of Catania) for the facilities and willingness shown during the activities; to G. S. Cassarino, geologist and former Director of the Regional Museum of Asphalt of Castelluccio and Tabuna and of the Archaeology O.U. of the Superintendence of Ragusa, for providing some photographic material, and, finally, to Lucia Mancini (ZAG, Slovenia) and to Sandro Donato (University of Calabria) for their help in image processing and analysis. Technical data on mechanical properties provided by Salvatore Tricomi (formerly A.B.C.D. mining Society) are greatly acknowledged.

Funding

This work was supported by the UNICT University Grant 2020/2022 (Pia.ce.ri.) Linea 2, for the following projects: 1) "*From rifting to continental collision: structural stratigraphic study of the Iblean surface and subsurface, geological and natural heritage of southeastern Sicily*" (DATASET Resp. R. Maniscalco); 2) "*Geomatic applications and petromatics: the new frontier of investigations from macro to micro scale*" (GEOPETROMAT, Resp. G. Ortolano). Measurements at Elettra Sincrotrone were carried out as part of Proposal 20195100 "*Investigation on porosity and permeability of asphalt bearing limestones from the Noto Formation (South-east Sicily, Italy)*". Scientific responsible: R. Punturo.

The paper is the result of cooperation between all of the Authors. Here we specify some specific assignments. Conceptualization: R.P., R. C., R.M.; Data curation: R.P., E.F., V.I.; Formal analysis: A.B., G.L., R.P., E.F., L.M.; Funding acquisition: R. P., R.M.; Investigation: R.P., R.M., A. B., G.L.; Methodology: R.P., A.B.; Supervision: R.P. and R.M.; Validation R.P., R. M. and R.C.

References

[1] C. Giavarini, P. Rovigatti, C. Zipelli, L'asfalto italiano - The Italian Asphalt, SITEBSi srl - Rassegna del bitume n. 45/03. (2003) 21–27.
[2] A. Kadkhodaie-Ilkhchi, H. Rahimpour-Bonab, M. Rezaee, A committee machine with intelligent systems for estimation of total organic carbon content from petrophysical data: An example from Kangan and Dalan reservoirs in South Pars Gas Field, Iran, Comput. Geosci. 35 (2009) 459–474, https://doi.org/10.1016/j.cageo.2007.12.007.
[3] A.G. Pellegrino, R. Maniscalco, F. Speranza, C. Hernandez-Moreno, G. Sturiale, Paleomagnetism of the Hyblean Plateau, Sicily: a review of the existing data set and new evidence of block rotation from the Scicli-Ragusa Fault System, Ital. J. Geosci. 135 (2016) 300–307, https://doi.org/10.3301/IJG.2015.30.
[4] C. Fianchino, Le pietre nell'architettura, Quaderni I.D.A.U. (1988) 117-122.
[5] S. Tricomi, La roccia asfaltica. I selaci. Il petrolio, Mineraria CNPI. (2004) 45–50.
[6] R. Punturo, R. Maniscalco, G. Cassarino, La "pietra pece" di Ragusa - Una roccia semplice che ha fatto molta strada, Bollettino CAI - Comitato Scientifico Centrale. (2021) 55–73.
[7] P.P.G. Orsi, Ragusa (Hybla Heraia) Di alcuni sepolcri spettanti all'arcaica necropoli e di altre minori scoperte, Atti Della R. Accademia Dei Lincei. Notizie Degli Scavi. (1892) 321–332.
[8] P.P.G. Orsi, Nuove esplorazioni nella necropoli di Hybla Heraea, Atti Della R. Accademia Dei Lincei. Notizie Degli Scavi. (1899) 402–418.
[9] S. Imposa, S. Grassi, I. Barone, M. Censini, G. Morreale, Combined GPR and seismic refraction tomography to study the subsoil in the Cathedral of S. Giorgio Ragusa-Ibla (Sicily), in: 2021 11th International Workshop on Advanced Ground Penetrating Radar (IWAGPR), IEEE, Valletta, Malta, 2021: pp. 1–3. https://doi.org/10.1109/IWAGPR50767.2021.9843154.
[10] S. Branca, R. Azzaro, E. De Beni, D. Chester, A. Duncan, Impacts of the 1669 eruption and the 1693 earthquakes on the Etna Region (Eastern Sicily, Italy): An example of recovery and response of a small area to extreme events, J. Volcanol. 303 (2015) 25–40, https://doi.org/10.1016/j.jvolgeores.2015.07.020.
[11] R. Punturo, L.G. Russo, A.L. Giudice, P. Mazzoleni, A. Pezzino, Building stone employed in the historical monuments of Eastern Sicily (Italy). An example: the ancient city centre of Catania, Environ. Geol. 50 (2006) 156–169, https://doi.org/10.1007/s00254-006-0195-3.
[12] Late Baroque Towns of the Val di Noto (South-Eastern Sicily) https://whc.unesco.org/en/documents/141487, (n.d.).
[13] https://www.unesco.it/it/PatrimonioMondiale/Detail/137, (n.d.).
[14] G. Barone, M.F. La Russa, A. Lo Giudice, P. Mazzoleni, A. Pezzino, The Cathedral of S. Giorgio in Ragusa Ibla (Italy): characterization of construction materials and their chromatic alteration, Environ. Geol. 55 (2008) 499–504, https://doi.org/10.1007/s00254-007-0995-0.
[15] R. Punturo, C. Ricchiuti, M. Rizzo, E. Marrocchino, Mineralogical and microstructural features of namibia marbles: insights about tremolite related to natural asbestos occurrences, Fibers 7 (2019) 31, https://doi.org/10.3390/fib7040031.
[16] R. Punturo, L.G. Russo, A. Lo Giudice, P. Mazzoleni, A. Pezzino, C. Trovato, S.C. Vinciguerra, I materiali lapidei utilizzati nei monumenti d'epoca tardo barocca del centro storico di Catania: caratterizzazione e degrado, in: Proceedings of the Workshop: L'approccio Multidisciplinare Ballo Studio e Alla Valorizzazione Dei Beni Culturali, Siracusa, 2005: pp. 347–356.
[17] G. Iurato, Un punto d'incontro fra il pensiero epistemologico di Felice Ippolito e l'archeologia industriale, nella disamina di alcune strutture ipogee iblee, Hal-01063823. (2014). https://hal.archives-ouvertes.fr/hal-01063823.
[18] G. Barone, E. Campani, A. Casoli, M.F. La Russa, A. Lo Giudice, P. Mazzoleni, A. Pezzino, The Cathedral of St. Giorgio in Ragusa Ibla (Italy): a case study of the use of protective products, Environ. Geol. 54 (2008) 1501–1506, https://doi.org/10.1007/s00254-007-0931-3.
[19] G. Barone, C. Calabrò, R. Cirrincione, G.M. Crisci, M.F. La Russa, P. Mazzoleni, S. A. Ruffolo, A. Pezzino, Characterization of stone materials and degradation forms

on the façade of St. Giuseppe in Ortigia (Italy): A case study, Rend, Online Soc. Geol. Ital. 3 (2008) 67–68.
[20] V. Cicero, La pietra nelle esperienze costruttive del territorio degli Iblei, dopo il terremoto del 1693, Archivum Historicum Mothycense 6 (2000) 77–103.
[21] D. Zaccagna, A proposito dello Stato coltivatore di miniere, La Miniera Italiana (II, N° 5). Pp. 161-181. II (1918) 161–181.
[22] F. Lentini S. Carbone Istituto Superiore per la Protezione e la Ricerca Ambientale . Italien, Geologia della Sicilia: = Geology of Sicily, ISPRA, Istituto superiore per la protezione e la ricerca ambientale 2014 Roma.
[23] M.A. Varfolomeev, R.N. Nagrimanov, A.V. Galukhin, A.V. Vakhin, B.N. Solomonov, D.K. Nurgaliev, M.V. Kok, Contribution of thermal analysis and kinetics of Siberian and Tatarstan regions crude oils for in situ combustion process, J. Therm. Anal. 122 (2015) 1375–1384, https://doi.org/10.1007/s10973-015-4892-6.
[24] R. Cirrincione, E. Fazio, P. Fiannacca, G. Ortolano, A. Pezzino, R. Punturo, The Calabria-Peloritani Orogen, a composite terrane in Central Mediterranean; Its overall architecture and geodynamic significance for a pre-Alpine scenario around the Tethyan basin, Period. Mineral. (2015), https://doi.org/10.2451/2015PM0446.
[25] I.R. Finetti, A. Del Ben, Crustal Tectono-Stratigraphic Setting of the Pelagian Foreland from New CROP Seismic Data., in: CROP PRO-JECT: Deep Seismic Exploration of the Central Mediterranean and Italy, Finetti I.R. (Ed.), 1996: pp. 581–595.
[26] A. Yellin-Dror, M. Grasso, Z. Ben-Avraham, G. Tibor, The subsidence history of the northern Hyblean plateau margin, southeastern Sicily, Tectonophysics 282 (1997) 277–289, https://doi.org/10.1016/S0040-1951(97)00228-X.
[27] F. Ghisetti, L. Vezzani, Contribution of structural analysis to understanding the geodynamic evolution of the Calabrian arc (Southern Italy), J. Struct. Geol. 3 (1981) 371–381, https://doi.org/10.1016/0191-8141(81)90037-7.
[28] S. Catalano, G. De Guidi, G. Romagnoli, S. Torrisi, G. Tortorici, L. Tortorici, The migration of plate boundaries in SE Sicily: Influence on the large-scale kinematic model of the African promontory in southern Italy, Tectonophysics 449 (2008) 41–62, https://doi.org/10.1016/j.tecto.2007.12.003.
[29] P.F. Burollet, J.M. Mugniot, P. Sweeney, The Geology of the Pelagian Block: The Margins and Basins off Southern Tunisia and Tripolitania, in: A.E.M. Nairn, W.H. Kanes, F.G. Stehli (Eds.), The Ocean Basins and Margins, Springer US, Boston, MA, 1978: pp. 331–359. https://doi.org/10.1007/978-1-4684-3039-4_6.
[30] A. Cilona, F. Agosta, A. Criscenti, G. Deiana, G. Giunta, G. Napoli, P. Renda, E. Tondi, Preliminary results of fault-related permeability structures associated to the Scicli-Ragusa fault segments, Hyblean Plateau, Sicily, Rend. Online Soc. Geol. Ital. 10 (2010) 35–38.
[31] F. Ghisetti, L. Vezzani, The structural features of the Iblean Plateau and of the Mount Judica area (southeastern Sicily); a microtectonic contribution to the deformational history of the Calabrian Arc, Boll. Soc. Geol. It. 99 (1980) 57–102.
[32] R. Maniscalco, E. Fazio, R. Punturo, R. Cirrincione, A. Di Stefano, S. Distefano, M. Forzese, G. Lanzafame, G.S. Leonardi, S. Montalbano, A.G. Pellegrino, A. Raele, G. Palmeri, The Porosity in Heterogeneous Carbonate Reservoir Rocks: Tectonic versus Diagenetic Imprint—A Multi-Scale Study from the Hyblean Plateau (SE Sicily, Italy), Geosciences. 12 (2022) 149, https://doi.org/10.3390/geosciences12040149.
[33] A. Bonforte, S. Catalano, R. Maniscalco, F. Pavano, G. Romagnoli, G. Sturiale, G. Tortorici, Geological and geodetic constraints on the active deformation along the northern margin of the Hyblean Plateau (SE Sicily), Tectonophysics 640–641 (2015) 80–89, https://doi.org/10.1016/j.tecto.2014.11.024.
[34] H.M. Pedley, G. Cugno, M. Grasso, Gravity slide and resedimentation processes in a Miocene carbonate ramp, Hyblean Platcau, southeastern Sicily, Sedimentary Geol. 79 (1992) 189–202, https://doi.org/10.1016/0037-0738(92)90011-F.
[35] S.V. Georgiev, H.J. Stein, J.L. Hannah, R. Galimberti, M. Nali, G. Yang, A. Zimmerman, Re–Os dating of maltenes and asphaltenes within single samples of crude oil, Geochim. Cosmochim. Acta 179 (2016) 53–75, https://doi.org/10.1016/j.gca.2016.01.016.
[36] S. Scirè, E. Ciliberto, C. Crisafulli, V. Scribano, F. Bellatreccia, G.D. Ventura, Asphaltene-bearing mantle xenoliths from Hyblean diatremes, Sicily, Lithos 125 (2011) 956–968, https://doi.org/10.1016/j.lithos.2011.05.011.
[37] M. Dipasquale, R. Occhipinti, Studio geologico strutturale preliminare di Contrada Tabuna (bacino asfaltifero di Ragusa, Sicilia), Rend. Online Soc. Geol. Ital. 12 (2010) 40–55.
[38] Miimageview, (2019). https://www.microdemo.com/product/goods/software/imageview/.
[39] E. Maire, P.J. Withers, Quantitative X-ray tomography, Int. Mater. 59 (2014) 1–43, https://doi.org/10.1179/1743280413Y.0000000023.
[40] D. Paganin, S.C. Mayo, T.E. Gureyev, P.R. Miller, S.W. Wilkins, Simultaneous phase and amplitude extraction from a single defocused image of a homogeneous object, J. Microsc. 206 (2002) 33–40, https://doi.org/10.1046/j.1365-2818.2002.01010.x.
[41] J. Schindelin, I. Arganda-Carreras, E. Frise, V. Kaynig, M. Longair, T. Pietzsch, S. Preibisch, C. Rueden, S. Saalfeld, B. Schmid, J.-Y. Tinevez, D.J. White, V. Hartenstein, K. Eliceiri, P. Tomancak, A. Cardona, Fiji: an open-source platform for biological-image analysis, Nat. Methods 9 (2012) 676–682, https://doi.org/10.1038/nmeth.2019.
[42] F. Brun, L. Mancini, P. Kasae, S. Favretto, D. Dreossi, G. Tromba, Pore3D: A software library for quantitative analysis of porous media, Nucl. 615 (2010) 326–332, https://doi.org/10.1016/j.nima.2010.02.063.
[43] A. Aboulhassan, F. Brun, G. Kourousias, G. Lanzafame, M. Voltolini, A. Contillo, L. Mancini, PyPore3D: an open source software tool for imaging data processing and analysis of porous and multiphase media, J. Imaging 8 (2022) 187, https://doi.org/10.3390/jimaging8070187.
[44] G. Lanzafame, F. Casetta, P.P. Giacomoni, S. Donato, L. Mancini, M. Coltorti, T. Ntaflos, C. Ferlito, The Skaros effusive sequence at Santorini (Greece): Petrological and geochemical constraints on an interplinian cycle, Lithos. 362–363 (2020), 105504, https://doi.org/10.1016/j.lithos.2020.105504.
[45] VGStudio, (2022). https://www.volumegraphics.com/en/products/vgstudio.html.
[46] F.S. Kadhim, A. Samsuri, A.K. Idris, H. Alwan, M. Hashim, Investigation of petrophysical properties for yamamma carbonate formation, MAS 9 (2015), p36, https://doi.org/10.5539/mas.v9n6p36.
[47] F.S. Kadhim, A.M. Imran, Y.F. Rasool, Using NMR, core analysis, and well logging data to predict permeability of carbonate reservoirs: a case study, IOP Conf. Ser.: Mater. Sci. Eng. 671 (1) (2020) 012071.
[48] ASTM, D 2845- 2000 indications, ASTM Standards on Disc, Vol. 04.08. Standard Test Method for Laboratory Determination of Pulse Velocities and Ultrasonic Elastic Constants of Rock, (2008).
[49] F.S. Birch, The velocity of compressional waves in rocks to 10 kilobars: Part 1, J. Geophys. 65 (1960) 1083–1102.
[50] D. Miriello, A. Bloise, G.M. Crisci, E. Barrese, C. Apollaro, Effects of milling: a possible factor influencing the durability of historical mortars, Archaeometry (2009), https://doi.org/10.1111/j.1475-4754.2009.00494.x.
[51] J.S. Caine, J.P. Evans, C.B. Forster, Fault zone architecture and permeability structure, Geol. 24 (1996) 1025, https://doi.org/10.1130/0091-7613(1996)024<1025:FZAAPS>2.3.CO;2.
[52] M. Zambrano, E. Tondi, L. Mancini, F. Arzilli, G. Lanzafame, M. Materazzi, S. Torrieri, 3D Pore-network quantitative analysis in deformed carbonate grainstones, Mar. Pet. Geol. 82 (2017) 251–264.
[53] J.P. Evans, C.B. Forster, J.V. Goddard, Permeability of fault-related rocks, and implications for hydraulic structure of fault zones, J. Struct. Geol. 19 (1997) 1393–1404, https://doi.org/10.1016/S0191-8141(97)00057-6.
[54] A. Aydin, Fractures, faults, and hydrocarbon entrapment, migration and flow, Marine Petrol. Geol. 17 (2000) 797–814, https://doi.org/10.1016/S0264-8172(00)00020-9.
[55] O. Bour, P. Davy, On the connectivity of three-dimensional fault networks, Water Resour. Res. 34 (1998) 2611–2622, https://doi.org/10.1029/98WR01861.
[56] R.J. Dunham, Classification of carbonate rocks according to depositional texture, in: Classification of Carbonate Rocks, Ham W. E., 1962: pp. 108–121.
[57] R.L. Folk, Practical petrographic classification of limestones, Am. Assoc. Pet. Geol. Bull. 43 (1959) 1–38.
[58] G. Afanasova, I. Shkhiyants, N. Nechitailo, V. Sher, P. Sanin, Study of oxidation of hydrocarbons by thermographic analysis, Petrol. Chem. U.S.S.R. 15 (1975) 220–226, https://doi.org/10.1016/0031-6458(75)90004-0.
[59] M.L.A. Gonçalves, M.A.G. Teixeira, R.C.L. Pereira, R.L.P. Mercury, J.R. Matos, Contribution of thermal analysis for characterization of asphaltenes from brazilian crude oil, J. Therm. Anal. 64 (2001) 697–706, https://doi.org/10.1023/A:1011588226768.
[60] P.D. Hopkins, Metal-catalyzed autoxidation of hydrocarbons studied by differential thermal analysis, IEC Prod. Res. Dev. (Online) 6 (1967) 246–253, https://doi.org/10.1021/i360024a010.
[61] I. Tijunelyte, N. Dupont, I. Milosevic, C. Barbey, E. Rinnert, N. Lidgi-Guigui, E. Guenin, M.L. de la Chapelle, Investigation of aromatic hydrocarbon inclusion into cyclodextrins by Raman spectroscopy and thermal analysis, Environ. Sci. Pollut. Res. 24 (2017) 27077–27089, https://doi.org/10.1007/s11356-015-4361-6.
[62] C.M. Schmidt, K. Heide, Thermal analysis of hydrocarbons in Paleozoic black shales, J. Therm. Anal. 64 (2001) 1297–1302, https://doi.org/10.1023/A:1011530020564.
[63] S. Gambino, E. Fazio, R. Maniscalco, R. Punturo, G. Lanzafame, G. Barreca, R.W. H. Butler, Fold-related deformation bands in a weakly buried sandstone reservoir analogue: A multi-disciplinary case study from the Numidian (Miocene) of Sicily (Italy), J. Struct. Geol. 118 (2019) 150–164, https://doi.org/10.1016/j.jsg.2018.10.005.
[64] M.F. La Russa, G. Barone, P. Mazzoleni, A. Pezzino, G.M. Crisci, M. Malagodi, G. Areddia, A. Vindigni, Il duomo di S. Giorgio a Ragusa Ibla: individuazione dei materiali litici utilizzati, implicazioni architettoniche ed analisi delle forme di degrado, in: C.RI.BE.CU.M., Siracusa, 2005.
[65] L. Anania, A. Badalà, G. Barone, C.M. Belfiore, C. Calabrò, M.F. La Russa, P. Mazzoleni, A. Pezzino, The stones in monumental masonry buildings of the “Val di Noto” area: New data on the relationships between petrographic characters and physical–mechanical properties, Constr. Build. Mater. 33 (2012) 122–132, https://doi.org/10.1016/j.conbuildmat.2011.12.076.
[66] M.F. La Russa, C.M. Belfiore, G.V. Fichera, R. Maniscalco, C. Calabrò, S.A. Ruffolo, A. Pezzino, The behaviour to weathering of the Hyblean limestone in the Baroque architecture of the Val di Noto (SE Sicily): An experimental study on the “calcare a lumachella” stone, Constr. Build. Mater. 77 (2015) 7–19, https://doi.org/10.1016/j.conbuildmat.2014.11.073.
[67] G. Cultrone, E. Sebastián, M.O. Huertas, Durability of masonry systems: A laboratory study, Constr. Build. Mater. 21 (2007) 40–51, https://doi.org/10.1016/j.conbuildmat.2005.07.008.
[68] A. Boeri, Pietre naturali nelle costruzioni: requisiti, criteri progettuali, applicazione, prestazioni, Hoepli, Milano, 1996.
[69] https://ec.europa.eu/environment/green-growth/resource-efficiency/index_en.htm, (2022).